Available online at www.sciencedirect.com
SCIENCE DIRECT®
International Journal of Heat and Mass Transfer 48 (2005) 2684–2696
International Journal of HEAT and MASS TRANSFER
www.elsevier.com/locate/ijhmt

Predicting the thermal performance characteristics of staggered vertical pin fin array heat sinks under combined mode radiation and mixed convection with impinging flow

C.J. Kobus *, T. Oshio

School of Engineering and Computer Science, Oakland University, Rochester, MI 48309-4401, USA

Received 10 December 2004; received in revised form 31 January 2005
Available online 21 March 2005

Abstract

A theoretical and experimental study was carried out investigating the influence of thermal radiation on the thermal performance of a pin fin array heat sink with the purpose of developing accurate predictive capability for such situations, and to determine the particular design parameters and environmental conditions under which thermal radiation might be advantageous to the thermal performance. Several different types of experimental tests were run with the corresponding physical parameter variations including the emissivity of the heat sink, elevated ambient air temperature, the temperature of a visible hot surface, and its radiation configuration factor. A theoretical model, validated by experimental data, which includes the capability of predicting the influence of thermal radiation on the thermal performance of a pin fin array heat sink, was developed by introducing an effective radiation heat transfer coefficient that was added to the convective heat transfer coefficient.

Keywords: Mixed; Combined; Convection; Radiation; Heat transfer

1. Introduction

Electronic component cooling becomes a more serious design problem as power densities continue to increase. One of the most common means for cooling electronic modules is a finned heat sink that enhances convection heat transfer to the ambient air. There are a variety of heat sink types, with differing fin geometries, and operating with natural or forced convection. A common geometry is a pin fin array heat sink. Most of the archival literature [1–10] on the thermal performance of a pin fin array heat sink only involve convective heat transfer, the reason being that the heat sink is often exposed to a cool air-stream. For this situation, forced convection is considered to be the dominant heat transfer mechanism. Since the magnitude of thermal radiation is normally very small compared to that of forced convection, thermal radiation is normally considered to be negligible. However, there are situations where the effects of thermal radiation are not negligible. An example would be when the air velocity is low enough such that the effects of thermal radiation and natural convection are the same order of magnitude as that of

* Corresponding author. Tel.: +1 248 370 2489; fax: +1 248 370 4416.
E-mail address: cjkobus@oakland.edu (C.J. Kobus).

0017-9310/$ - see front matter © 2005 Elsevier Ltd. All rights reserved.
doi:10.1016/j.ijheatmasstransfer.2005.01.016

Nomenclature

A	cross sectional area of fin, $\pi d^2/4$, m^2
A_b	base area not occupied by fins, $(ab - nA)$, m^2
A_c	total convective heat transfer area of fin array heat sink, $n(\pi dL) + (ab - nA)$, m^2
A_f	total effective radiation surface area of fin array heat sink, $ab + 2(a + b)L$, m^2
A_s	total radiation surface area of a hot surface, m^2
A_v	portion of the total effective radiation surface area of finned heat sink which is in view of a hot surface, ab, m^2
a	width of heat sink, m
b	length of heat sink, m
c_p	specific heat, J/kg-°C
d	fin diameter, m
$F_{A_v \to A_s}$	radiation configuration (view) factor between surface A_v and A_s
f_q	heat flux, W/m^2
f_{qr}	radiation heat flux, W/m^2
Gr_d	Grashof number
Gr_d^*	modified Grashof number, r^*Gr_d
h	convective heat transfer coefficient, W/m^2 °C
h_c	convective heat transfer coefficient between the fin and flowing air, W/m^2 °C
h_r^*	effective radiation heat transfer coefficient, W/m^2 °C
$h_{r,c}^*$	effective radiation heat transfer coefficient representing the influence of thermal radiation of the experimental data that were taken to develop the dimensionless correlation functions, W/m^2 °C
k	fin thermal conductivity, W/m °C
k_f	fluid thermal conductivity, W/m °C
L	length of fin, m
m	fin parameter, m^{-1}
n	number of fins
Nu_d	Nusselt number
P'	periphery of fin, m
P	electrical power, W
$\dot{Q}_s$	heat transfer from entire sink, W
r'	Reynolds number modifier
r^*	Grashof number modifier
Re_d	Reynolds number
Re_d'	modified Reynolds number, $r'Re_d$
$R_{t,s}$	effective thermal resistance, W/°C
T_b	base temperature, K
T_f	air temperature, K
T_s	hot surface temperature, K
v_f	free stream air velocity, m/s

Greek symbols

α	void fraction of fin bundle
β	coefficient of thermal expansion, K^{-1}
ε_b	heat sink emissivity
ε_s	hot surface emissivity
μ	dynamic viscosity, kg/m-s
ρ	air density, kg/m^3
ρ'	surface reflectivity
σ	Stefan–Boltzman constant, W/m^2 K^4

forced convection should any exist. Another example would be when the heat sink is exposed to a hot surface, such as might exist in some automotive applications. There appears to have been relatively very little research done on the effect of thermal radiation on heat sink performance as compared to that done considering just pure convection.

Rao and Venkateshan [11] carried out an experimental study on the interaction of natural convection and thermal radiation in horizontal fin arrays. A differential interferometer was used to measure natural convection heat transfer, and thermal radiation was calculated by numerically solving the integro-differential equations. The effect of thermal radiation between plate fins on the thermal performance of a fin array heat sink was discussed. Sparrow and Vemuri [12] carried out an experimental study on combined-mode natural convection/radiation heat transfer characteristics of highly populated arrays of pin fins. The effect of various parameters on the thermal performance was investigated. It was found that performance increased with fin length. The study revealed the existence of an optimum number of fins for a fixed base plate size. The contribution of radiation was determined to be substantial and was greatest for more populous arrays, for longer fins, and at small baseplate-to-ambient temperature differences. Sparrow and Vemuri [13] later extended their study to different orientations. Aihara et al. [14] carried out an experimental study on natural convection and radiation heat transfer from dense pin fin arrays with a vertical base plate. A numerical analysis was performed on the radiation heat transfer from a pin fin array heat sink. The average heat transfer coefficient was correlated by the Nusselt and Rayleigh numbers. Chapman et al. [6] carried out an experimental and theoretical study of the thermal performance of different types of fin array heat sinks.

A numerical thermal radiation model was included in the theoretical study. The effect of thermal radiation on thermal performance, however, was not fully discussed. More recently, Yu and Joshi [15] studied the combined mode convection/radiation heat transfer utilizing computational modeling, temperature measurements and flow visualization. Their study, based on their earlier research [16], however, was confined to an enclosure heated by discrete components. Sasikumar and Balaji [17] analyzed various design constraints on a convecting–radiating fin array standing vertically on the outside of a horizontal duct. Their fin array consisted of triangular, trapezoidal or rectangular profile fins with uniform depth. Pin fin arrays were not investigated in this prior research. Gerencser and Razani [18] did study the combined-mode convection/radiation from a pin fin array heat sink similar to [11], but assumed the fins were black and the pin fins themselves were tapered. It appears in this prior research that the heat sink orientation was horizontal and only natural convection was considered.

This limited information in the archival literature on the influence of thermal radiation on heat sink performance was the motivation for the current study. The purpose of the current research was to both theoretically and experimentally investigate the influence of thermal radiation on the thermal performance of a pin fin array heat sink. The theoretical model is formulated by introducing an effective radiation heat transfer coefficient which was added to the convective heat transfer coefficient. Of interest were the particular design parameters and environmental conditions under which thermal radiation could be either advantageous or detrimental to the thermal performance of the heat sink.

2. Formulation of theoretical thermal radiation model

A theoretical thermal radiation model is developed to predict the magnitude of the influence of thermal radiation on the thermal performance of heat sink fins. The intent of this modeling approach is to formulate the thermal radiation model in such a way that it complements the theoretical model already developed by Kobus and Oshio [10] for natural and combined forced and natural convection. This is done by developing an effective radiation heat transfer coefficient that can be directly added to the convective heat transfer coefficient obtained from the empirical convective heat transfer correlations to yield an effective total heat transfer coefficient.

3. Basic theoretical model

As summarized in the previous research [10], the effective thermal resistance of a pin fin array heat sink (Fig. 1), $R_{t,s}$, can be modeled as

$$R_{t,s} = \frac{(T_b - T_f)}{\dot{Q}_s} = \{n[kmA\tanh(mL)] + h(ab - nA)\}^{-1} \quad (1)$$

where

$$m = \left(\frac{hP'}{kA}\right)^{1/2} \quad (2)$$

The above equation represents a theoretical model for predicting the effective thermal resistance of the heat sink, $R_{t,s}$, in terms of the thermal conductivity of the fin material, k, fin diameter,[1] d, length, L, number of fins, n, area of the heat sink base, ab, and the convective heat transfer coefficient, h, between the fins and the flowing air. For simplicity, it was assumed that the convective heat transfer coefficient, h, is the same for each fin, and also for the base. It should be noted, however, that this value will include an average that is inclusive of the flow and thermal bundle effect that occurs within the array. Referring to Eq. (1), all of the physical and thermal parameters are readily obtainable, the exception being the convective heat transfer coefficient, h. The convective heat transfer coefficient is the result of a combination of a number of complex physical mechanisms involving fin geometry, fin spacing, free stream air velocity and direction, buoyancy forces, and fluid properties in addition to the bundle effect. The complexity of the physical mechanisms governing this particular physical parameter is such that they can only partially be modeled. Therefore, in order to determine the required convective heat transfer coefficient, h, for a fin-bundle, there will be the need for developing some form of empirical correlation from appropriate experimental data.

3.1. Fin geometry and air flow orientation

The parameters s_1 and s_2 represent fin spacing for the fin pattern shown in Fig. 1. The symbol, L, is the fin length. Gravitational and flow orientation[2] for the heat sink is also shown in Figs. 1 and 2. For pure natural convection, however, the air velocity is zero; $v_f = 0$.

3.2. Convective heat transfer correlation function

The dimensionless convective heat transfer coefficient correlation function is of the form:

$$\frac{Nu_d}{Pr^{1/3}} = f^*(Gr_d^*) + f'(Re_d') \quad (3)$$

[1] If the fin is tapered, the average diameter, d, is the arithmetic mean between the tip and the base diameter, $d = (d_t + d_b)/2$.

[2] All of the experimental data used in developing the correlation function are for the specific gravitational and airflow orientation shown in Fig. 2, with $D = 15.2$ cm.

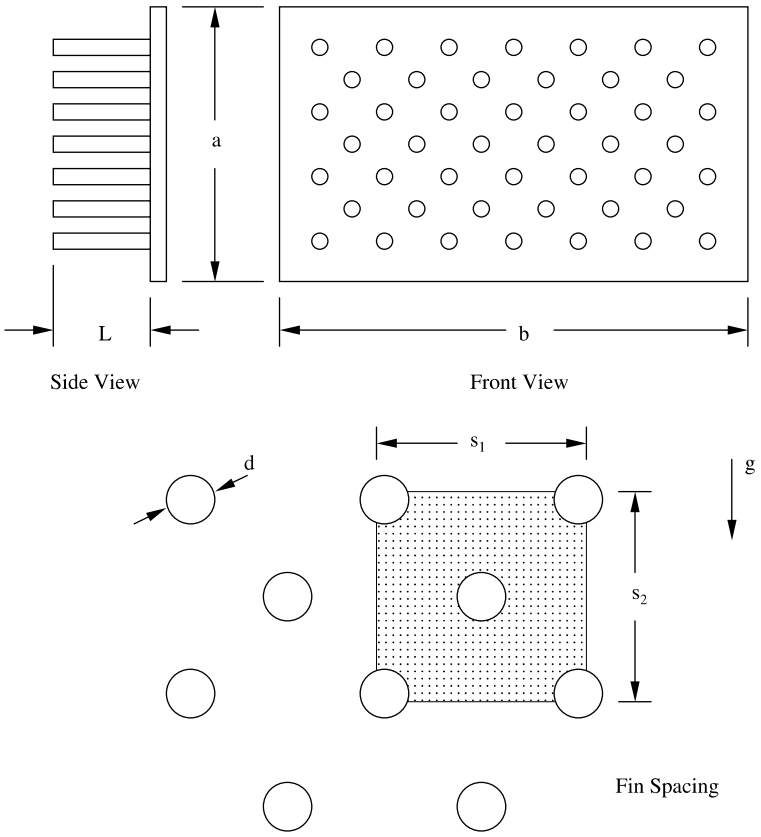

Fig. 1. Schematic of pin fin array heat sink and spacing.

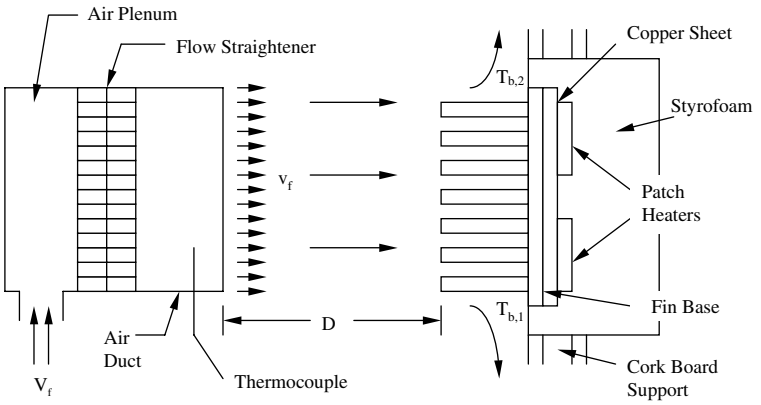

Fig. 2. Schematic of experimental test set-up.

where

$$f^*(Gr_d^*) = c_0^*(Gr_d^*)^{n^*} \tag{4}$$

$$f'(Re_d') = c_0 + c_1 Re_d' + c_2 Re_d'^2 + c_3 Re_d'^3 \tag{5}$$

$$Gr_d^* = r^* Gr_d = \text{modified Grashof number} \tag{6}$$

$$Re_d' = r' Re_d = \text{modified Reynolds number} \tag{7}$$

The dimensionless convective heat transfer coefficient, Nu_d, is the classic Nusselt number, and Pr is the classic Prandtl number. The modifiers r^* and r' involve fin void fraction, α, fin geometry, fin spacing and heat sink base height, and are determined empirically from an

experimental database. Gr_d and Re_d are the classical Grashof and Reynolds numbers, respectively; thus

$$Gr_d = \frac{\rho^2 g\beta(T_b - T_f)d^3}{\mu^2} \tag{8}$$

$$Re_d = \frac{\rho v_f d}{\mu} \tag{9}$$

$$\alpha = \left\{1 - \frac{2(\pi d^2/4)}{s_1 s_2}\right\}; \quad s_1 = s_2/2 \tag{10}$$

4. Effective total heat transfer coefficient

An effective total heat transfer coefficient, h, can be defined as the sum of the convective heat transfer coefficient obtained from the empirical convective heat transfer correlations, h_c, and the difference between the effective radiation heat transfer coefficient representing the influence of thermal radiation of the current situation of interest, h_r^*, and the effective radiation heat transfer coefficient, $h_{r,c}^*$, representing the influence of thermal radiation that is inherent[3] in the experimental data used to develop the empirical convective heat transfer correlations. Thus, the effective total heat transfer coefficient, h, can be expressed as

$$h = (h_c - h_{r,c}^*) + h_r^* = h_c + (h_r^* - h_{r,c}^*) \tag{11}$$

The reason for subtracting the effective radiation heat transfer coefficient, $h_{r,c}^*$, from that of the correlation, h_c, is to obtain a pure convective heat transfer coefficient, $(h_c - h_{r,c}^*)$. Then, by adding the effective radiation heat transfer coefficient for the current situation of interest, h_r^*, to the pure convective heat transfer coefficient, it is possible to determine the effective total heat transfer coefficient, h, for the current situation of interest.

5. Determination of convective heat transfer coefficient

The convective heat transfer coefficient, h_c, for a specific fin geometry and air velocity can be determined by rearranging Eq. (3), thus

$$Nu_d = Pr^{1/3}\left\{f^*(Gr_d^*) + f'(Re_d')\right\} \tag{12}$$

where

$$Nu_d = \frac{h_c d}{k_f} \tag{13}$$

$$Pr = \frac{\mu c_p}{k_f} \tag{14}$$

Therefore, the convective heat transfer coefficient, h_c, can be determined by combining Eqs. (12) and (13) as follows:

$$h_c = \frac{k_f}{d} Pr^{1/3}\{f^*(Gr_d^*) + f'(Re_d')\} \tag{15}$$

where $f^*(Gr_d^*)$ and $f'(Re_d')$ are determined from Eqs. (4) and (5) respectively. The modifiers r^*, r' and the coefficients c_0^*, n^* and c_0, c_1, c_2 and c_3 were obtained empirically by Kobus and Oshio [10] for a pin fin array heat sink with impinging flow, and are given as follows:

$$r^* = (1-\alpha)^{-1.9}\left(\frac{s_2}{a}\right)^{2.4}\left(\frac{s_1}{b}\right)^{1.4}\left(\frac{d}{L}\right)^{0.8}; \quad s_1 = s_2/2 \tag{16}$$

where α is the void fraction (Eq. (10)), and the coefficients c_0^* and n^* are given by

$$c_0^* = 1.141, \quad n^* = 0.230 \tag{17}$$

$$r' = \alpha^{2.1}\left(\frac{a}{s_2}\right)^{0.4}\left(\frac{L}{d}\right)^{0.1} \tag{18}$$

$$c_0 = -3.12 \times 10^{-2}, \quad c_1 = -2.99 \times 10^{-3},$$
$$c_2 = 1.46 \times 10^{-4}, \quad c_3 = -3.55 \times 10^{-7} \tag{19}$$

5.1. Domain of applicability for convective heat transfer correlation function

The dimensionless convective heat transfer correlation function that has been developed above has been shown to give good results for the specific gravitational and flow orientation shown in Fig. 2 where $D = 15.2$ cm. Also, the accuracy of the correlation has only been verified experimentally for the following range of fin, flow and heat sink parameters: $5.1 \leqslant a$, $b \leqslant 14.6$ cm, $1.3 \leqslant s_2 \leqslant 2.3$ cm, $2 \leqslant L \leqslant 4.5$ cm, $2.3 \leqslant d \leqslant 4.1$ mm, $0 \leqslant v_f \leqslant 0.61$ m/s.

6. Modeling the effective radiation heat transfer coefficient

6.1. Total effective thermal radiation surface area of heat sink fins

The total effective radiation surface area of heat sink fins, A_r, is defined as the outer projected surface area of heat sink fins. Thus, it can be expressed as

$$A_r = ab + 2(a+b)L \tag{20}$$

The reason the total effective thermal radiation surface area of the heat sink fins, A_r, includes only the outer projected surface area of the heat sink fins is because the internal fins inside of the heat sink essentially radiate

[3] This requires a knowledge of the conditions under which the empirical data was obtained; emissivity and temperature of the fins and base, and temperature of the surroundings.

to each other. It is assumed that only those heat sink fins that can view the outside environment radiate to that environment.

6.2. Different segments of thermal radiation from heat sink fins

There are three different segments of thermal radiation from the heat sink fins with respect to the various surfaces viewed by the fins. Fig. 3 shows these three different segments of the total thermal radiation. One segment is the thermal radiation between that portion of the total effective radiation area of the heat sink fins that is in view of a hot surface, A_v, and the hot surface area itself, A_s. The second segment is the thermal radiation between that portion of the total effective radiation area of the heat sink fins which is in view of a hot surface, A_v, and the rest of the environment, $(A_c - A_s)$. The last segment is the thermal radiation between that portion of the total effective radiation area of the heat sink fins that is not in view of a hot surface, $(A_r - A_v)$, and the environment, $(A_c - A_s)$. Thus, the net rate of thermal energy transfer from the heat sink to those areas by the mechanism of thermal radiation can be expressed as

$$\dot{Q}_{rad} = f_{qr,A_v\to A_s}A_v + f_{qr,A_v\to(A_c-A_s)}A_v + f_{qr,(A_r-A_v)\to(A_c-A_s)}A_v \quad (21)$$

where $f_{qr,A_v\to A_s}$, $f_{qr,A_v\to(A_c-A_s)}$ and $f_{qr,(A_r-A_v)\to(A_c-A_s)}$ are net thermal radiation heat fluxes between surfaces A_v and A_s, A_v and $(A_c - A_s)$, and $(A_r - A_v)$ and $(A_c - A_s)$, respectively. Also, the net rate of radiation heat transfer, $\dot{Q}_{rad}$, can be expressed in terms of an effective radiation heat transfer coefficient representing the influence of thermal radiation from the heat sink fins, h_r^*, the total convective heat transfer surface area of the heat sink fins, A_c, and the difference between the base temperature of the heat sink fins and that of the air, $(T_b - T_f)$, as[4]

$$\dot{Q}_{rad} = h_r^* A_c (T_b - T_f) \quad (22)$$

where

$$A_c = n(\pi dL) + (ab - n\pi d^2/4)$$

Substituting Eq. (21) into (22) and solving for h_r^* yields

$$h_r^* = \frac{f_{qr,A_v\to A_s}A_v + f_{qr,A_v\to(A_c-A_s)}A_v + f_{qr,(A_r-A_v)\to(A_c-A_s)}(A_f - A_v)}{A_c(T_b - T_f)} \quad (23)$$

6.3. Modeling the net thermal radiation heat flux

The net thermal radiation heat flux, $f_{qr,A_i\to A_j}$, between two arbitrary surfaces, A_i and A_j, can be modeled as

$$f_{qr,A_i\to A_j} = \frac{\varepsilon_i\varepsilon_j\sigma(T_i^4 - T_j^4)F_{A_i\to A_j}}{1 - \rho_i'\rho_j'F_{A_i\to A_j}F_{A_j\to A_i}} \quad (24)$$

Now, from Eq. (24), the net thermal radiation heat flux between the two surface areas, A_v and A_s, can be expressed as

$$f_{qr,A_v\to A_s} = \frac{\varepsilon_b\varepsilon_s\sigma(T_b^4 - T_s^4)F_{A_v\to A_s}}{1 - \rho_b'\rho_s'F_{A_v\to A_s}F_{A_s\to A_v}} \quad (25)$$

where ε_b, ρ_b', T_b are the emissivity, reflectivity and base temperature respectively of heat sink fins, respectively and ε_b, ρ_b', T_b are the emissivity, reflectivity and temperature respectively of hot surface, A_s, respectively. For a grey surface the reflectivity can be expressed in terms of emissivity as

$$\rho_i' = 1 - \varepsilon_i \quad (26)$$

Using the reciprocity relationship for diffuse radiation, the configuration factor between surface A_j and A_i can be expressed in terms of the radiation configuration factor between surface A_i and surface A_j; thus

$$F_{A_j\to A_i} = \left(\frac{A_i}{A_j}\right)F_{A_i\to A_j} \quad (27)$$

Substituting Eqs. (26) and (27) into (25) yields

$$f_{qr,A_v\to A_s} = \frac{\varepsilon_b\varepsilon_s\sigma(T_b^4 - T_s^4)F_{A_v\to A_s}}{1 - (1-\varepsilon_b)(1-\varepsilon_s)\left(\frac{A_v}{A_s}\right)F_{A_v\to A_s}^2} \quad (28)$$

Similarly, from Eq. (24), the net thermal radiation heat flux between the two surface areas, A_v and $(A_c - A_s)$, can be expressed as

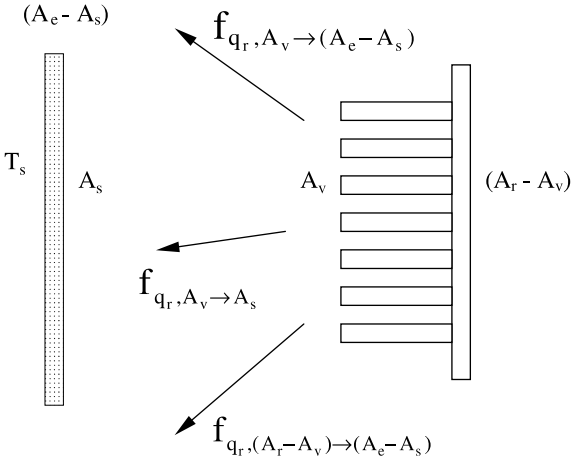

Fig. 3. Thermal radiation from pin fin array heat sink.

[4] This assumes the fin temperatures to be approximately equal to the base temperature, which would be true when the fin efficiency is approximately unity; a reasonable assumption for aluminum fins where forced convection is the same order of magnitude as natural convection.

$$f_{\mathrm{qr},A_v\to(A_c-A_s)}=\frac{\varepsilon_b\varepsilon_c\sigma(T_b^4-T_c^4)F_{A_v\to(A_c-A_s)}}{1-\rho'_b\rho'_cF_{A_v\to(A_c-A_s)}F_{(A_c-A_s)\to A_v}} \tag{29}$$

where ε_e, ρ'_e and T_e are the emissivity, reflectivity and temperature of the environment, respectively. As shown in Fig. 3, surface A_v only sees the hot surface, A_s, and the rest of the environment, $(A_e - A_s)$. Therefore, the following relationship exists between the radiation configuration factors:

$$F_{A_v\to A_s}+F_{A_v\to(A_e-A_s)}=1 \tag{30}$$

Also, it is assumed that nothing is reflected back to the heat sink fins from the environment since the various surfaces in the environment are assumed to be of low reflectivity, and are facing many different directions. Therefore, the reflectivity of the environment, ρ'_e, is assumed to be zero, which means from Eq. (26) that the emissivity of the environment, ε_e, is assumed to be unity. Moreover, the temperature of the environment, T_e, is assumed to be essentially equal to the air temperature, T_f. Therefore, using Eq. (30), Eq. (29) becomes

$$f_{\mathrm{qr},A_v\to(A_c-A_s)}=\varepsilon_b\sigma(T_b^4-T_c^4)(1-F_{A_v\to A_s}) \tag{31}$$

Similarly, from Eq. (24), the net thermal radiation heat flux between the two surface areas, $(A_r - A_v)$ and $(A_e - A_s)$, can be expressed as

$$f_{\mathrm{qr},(A_r\to A_v)\to(A_e-A_s)}=\frac{\varepsilon_b\varepsilon_e\sigma(T_b^4-T_e^4)F_{(A_r\to A_v)\to(A_e-A_s)}}{1-\rho'_b\rho'_eF_{(A_r\to A_v)\to(A_e-A_s)}F_{(A_e-A_s)\to(A_r\to A_v)}} \tag{32}$$

As shown in Fig. 3, the radiation configuration factor between surface $(A_r - A_v)$ and surface $(A_e - A_s)$ is unity. Also as explained above, the reflectivity of the environment, ρ_e, is zero, and the emissivity of the environment, ρ_e, is unity. The temperature of the environment, T_e, is essentially equal to the air temperature, T_f. Therefore, Eq. (32) becomes

$$f_{\mathrm{qr},(A_r\to A_v)\to(A_e-A_s)}=\varepsilon_b\sigma(T_b^4-T_f^4) \tag{33}$$

Substituting Eqs. (28), (31) and (33) into Eq. (23) and rearranging, yields

$$h_r^*=\left\{\frac{\left(\frac{A_v}{A_e}\right)\varepsilon_b\varepsilon_s\sigma F_{A_v\to A_s}}{1-(1-\varepsilon_b)(1-\varepsilon_s)\left(\frac{A_v}{A_s}\right)F_{A_v\to A_s}^2}\right\}\frac{(T_b^4-T_s^4)}{(T_b-T_f)}+\frac{\varepsilon_b\sigma}{A_e}(A_r-A_vF_{A_v\to A_s})(T_b+T_f)(T_b^2+T_f^2) \tag{34}$$

Eq. (34) expresses the effective radiation heat transfer coefficient representing the influence of the total thermal radiation from the finned heat sink. The effective radiation heat transfer coefficient, $h^*_{r,c}$, representing the influence of thermal radiation of the heat sink fins during the experimental tests, from which the empirical convective heat transfer correlations were developed, can be deduced from Eq. (34). Since there was no hot surface present when those experimental tests were run, the radiation configuration factor, $F_{A_v\to A_s}$ was zero, and the emissivity of the fins, ε_b, during those tests was $\varepsilon_{b,c}$. Therefore, in this case, Eq. (34) reduces to

$$h^*_{r,c}=\left(\frac{A_r}{A_c}\right)\varepsilon_{b,c}\sigma(T_b+T_f)(T_b^2+T_f^2) \tag{35}$$

Eq. (35) depicts the effective radiation heat transfer coefficient representing the influence of thermal radiation of the fin array heat sink during the experimental tests that were used to develop the dimensionless correlations. Therefore, temperatures T_b and T_f should be the values used when developing the correlations. Substituting Eqs. (34) and (35) into Eq. (11), an effective total heat transfer coefficient, h, can be determined that now includes the influence of thermal radiation. Using this effective total heat transfer coefficient, h, in Eqs. (1) and (2), the effective thermal resistance of a heat sink, $R_{t,s}$, can be predicted for the situation where the influence of thermal radiation is taken into consideration.

6.4. Domain of applicability for effective radiation heat transfer coefficient

The theoretical model for the effective radiation heat transfer coefficient, expressed by Eq. (34), has only been verified experimentally for the following range of thermal radiation parameters: $21.1 \leqslant T_f \leqslant 63.3$ °C, $(T_b - T_f) = 15$ °C, $-8.3 \leqslant T_s \leqslant 198$ °C, $0.1 \leqslant \varepsilon \leqslant 0.88$, $0 \leqslant F_{A_v\to A_s} \leqslant 0.55$.

7. Experimental verification of modified theoretical model including thermal radiation effects

The primary purpose of this section is to validate the predictive capability of the modified theoretical model that includes the influence of thermal radiation by comparison with experimental data of the model's prediction of the effective thermal resistance, $R_{t,s}$, as a function of air velocity, v_f. The basic model of the heat sink is given by Eq. (1), and the correlation function for the convective heat transfer coefficient, h_c, is given by Eq. (15). However, as shown in Eq. (11), the effective radiation heat transfer coefficient, $(h_r - h^*_{r,c})$, must be added to the convective heat transfer coefficient to determine the effective total heat transfer coefficient, h, as a result of taking the influence of thermal radiation into consideration, Eqs. (34) and (35). The other purpose of this section is to show the effect thermal radiation on the thermal performance of the heat sink by investigating the influence of various radiation parameters such as ambient and surface temperatures, emissivities, and radiation configuration factors. The experimental apparatus and measurement techniques used here are the

same as those described in an earlier paper [10]. Since the prior research discussed the experimental procedure and associated experimental uncertainties, they will not be repeated here.

7.1. Influence of fin emissivity on thermal performance of heat sink fins

In order to gain physical insight into the influence of fin emissivity, ε_b, on heat sink performance, two normal experimental tests were run (Fig. 2 with $D = 15.2$ cm and T_f approximately 21 °C) measuring the effective thermal resistance, $R_{t,s}$, as a function of air velocity, v_f. The heat sink that was tested was the smaller size that had a vertical base height, $a = 5.4$ cm, and a base width, $b = 12.4$ cm. The heat sink fin parameters were diameter, $d = 3.2$ mm, length, $L = 3.2$ cm, fin spacing, $s_2 = 1.8$ cm, and the number of fins, $n = 76$. The only difference in the two tests was the fin emissivity. In the first test, the fins had a polished aluminum surface, $\varepsilon = 0.1$. In the second test, the fins had a flat black painted surface, $\varepsilon = 0.88$. Emissivity measurements were made using an infrared sensor accurate to ±5% of the reading.

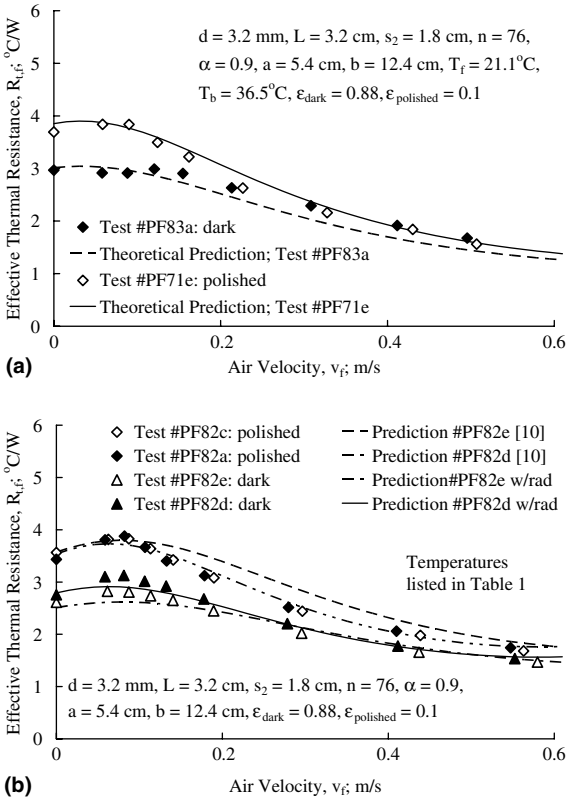

Fig. 4. Radiation effects on the thermal performance of a pin fin array heat sink; (a) influence of fin emissivity, (b) influence of elevated temperature and fin emissivity.

Fig. 4a depicts the experimentally measured thermal performance of the fin array heat sink along with the predictions of the theoretical model. As can be seen, the agreement between the predictions and the experimental data is quite good. There is not much difference in the thermal performances for the higher air velocities ($v_f \geqslant 0.24$ m/s). This makes physical sense because the heat transfer mechanism at the higher air flow is dominated by forced convection. Since the magnitude of the thermal radiation heat flux is small compared to the magnitude of the forced convection heat flux, thermal radiation does not have much influence. However, at the lower air velocity ($v_f < 0.24$ m/s), the dark heat sink fins ($\varepsilon_b = 0.88$) performed considerably better than the polished aluminum heat sink fins ($\varepsilon_b = 0.1$). Here, the graph clearly shows the influence of thermal radiation. The reason is because, at the lower air velocity, natural convection plays an important role. Since natural convection heat fluxes are small in the natural convection domain ($v_f < 0.24$ m/s), the effects of thermal radiation can be better seen. In these two tests, two different emissivities (0.1 and 0.88) were chosen. Since the emissivity of the heat sink fins was the only parameter that was changed, the different results seen in Fig. 4a are due solely to the influence of emissivity. Note that for the emissivity, $\varepsilon_b = 0.88$, and the case where forced convection was negligible, $v_f < 0.1$ m/s, the contribution of thermal radiation was at least 30% of the contribution of natural convection. This was the same order of magnitude found by Sparrow and Vemuri [12].

7.2. Influence of elevated air temperature and fin emissivity on thermal performance of heat sink fins

In order to investigate the influence of elevated air temperature and fin emissivity on the thermal performance of heat sink fins, four tests were run in an isothermal enclosure, which could be maintained at the elevated temperature (walls, air and other contents), measuring the effective thermal resistance, $R_{t,s}$, as a function of air velocity, v_f. The heat sinks that were tested were the exact same ones which were used in the emissivity tests described in the previous section. The heat sink and the air duct were set inside of the isothermal enclosure. Airflow orientation was the same direction as that shown in Fig. 2, but where $D = 7.0$ cm.[5] The first test was run using the polished aluminum surface heat sink fins ($\varepsilon_b = 0.1$) with the air temperature at normal room temperature. This was done to get a baseline for the thermal performance of the heat sink fins within the isothermal enclosure for the slightly modified

[5] The reason the distance, D, was not the usual 15.24 cm was due to the fact that there was limited space available within the isothermal enclosure.

airflow orientation. The second test was run with the air at an elevated temperature. The same two tests were repeated for the dark heat sink fins ($\varepsilon_b = 0.88$); one with the air temperature at normal room temperature, and the other at an elevated temperature. The highest elevated temperature that could be obtained within the enclosure without damaging various components of the experimental apparatus was $T_f = 63$ °C.

A comparison of the thermal performance of the heat sink fins having the two different emissivities, $\varepsilon_b = 0.1$ and $\varepsilon_b = 0.88$ for the two different air temperatures, $T_f = 22.8$ °C and $T_f = 63.1$ °C, is shown in Fig. 4b. As can be seen from the graph of the experimental data, there is not much difference in the thermal performance, with or without the elevated air temperature, for the polished aluminum heat sink fins ($\varepsilon_b = 0.1$). However, for the dark heat sink fins ($\varepsilon_b = 0.88$), the thermal performance at the elevated air temperature was considerably improved in the natural convection domain, $v_f < 0.18$ m/s. Also, with and without the elevated air temperature, the dark heat sink fins ($\varepsilon_b = 0.88$) performed much better than the polished aluminum heat sink fins ($\varepsilon_b = 0.1$). This also illustrates the influence of the fin emissivity. Moreover, the difference in the thermal performance of the polished aluminum heat sink fins ($\varepsilon_b = 0.1$) and the dark heat sink fins ($\varepsilon_b = 0.88$) is larger with the elevated air temperature than with the normal ambient air temperature. The reason is because the magnitude of thermal radiation heat flux is proportional to the difference between the fourth power of the absolute temperature of the heat sink base and that of the ambient air temperature respectively, $(T_b^4 - T_f^4)$. Therefore, the influence of thermal radiation on the thermal performance is larger with the elevated air temperature, even though the base to air temperature difference, $(T_b - T_f)$, remains the same.

The predictive capability of the modified theoretical model is also depicted in Fig. 4b, where the experimental data of these four tests are compared with the predictions of the model. Although there is some error in the magnitude, the model prediction shows the right trend, and the general agreement appears to be quite good, especially when consideration is given to the complexity of the various physical mechanisms involved: combined natural and forced convection as well as thermal radiation, both at normal and elevated temperatures.

7.3. Influence of a hot surface temperature on thermal performance of finned heat sink

With the experimental tests that have been shown thus far, there was no hot surface in view of the fin array heat sink. Therefore, the heat sink has been radiating only to the surfaces in the environment, which are at the ambient air temperature. In some situations, however, a hot surface might be in view of the heat sink. Such a situation might exist in automotive applications. Since the magnitude of the thermal radiation heat flux is proportional to the difference between the fourth power of the absolute temperature of the heat sink base and that of the hot surface temperature respectively, $(T_b^4 - T_s^4)$, it is important to investigate the influence of a hot surface temperature on the thermal performance of the heat sink.

7.4. Experimental considerations

The heat sink tested had a vertical base height, $a = 7.6$ cm, and a base width, $b = 14.6$ cm. The fin parameters were diameter, $d = 3.2$ mm, length, $L = 3.2$ cm, and fin spacing, $s_2 = 1.8$ cm. The number of fins was $n = 137$. The heat sink fin surfaces were dark ($\varepsilon_b = 0.88$). The fin spacing was the same as that of Fig. 1, with the dimension, s_1, being parallel with the base dimension, b.

A dark hot surface ($\varepsilon_s = 0.88$) that had a vertical base height of 7.6 cm and a base width of 15.2 cm was set in front of the fin array heat sink as shown in Fig. 3. It was heated with two 2.54 cm × 10.2 cm electrical patch heaters. The tests were only run with pure natural convection, $v_f = 0$ m/s, measuring the effective thermal resistance, $R_{t,s}$, as a function of the hot surface temperature, T_s, since the influence of thermal radiation on the thermal performance of the heat sink fins would be the greatest in the natural convection domain. In order to investigate the influence of the hot surface temperature on the thermal performance of the heat sink fins, the tests were run with eight different hot surface temperatures, ranging between, $-48.3\ °C \leqslant T_s \leqslant 204.4\ °C$, while the radiation view factor, $F_{A_v \to A_s}$, was kept constant by holding the distance and orientation between the hot surface and the tip of the fin array heat sink constant. Although this would be rare, it should be noted that two of the tests were run with the hot surface temperature being lower than that of the ambient air temperature, 21.1 °C, in an effort to verify the theoretical model over a larger temperature domain.

7.5. Determination of the radiation view factors

One of the difficulties with the thermal radiation test is the determination of the radiation configuration factors. After a careful study, it was concluded that the best way of handling the radiation view factor was to use a simple geometry, where theoretical models for expressing the view factors have already been developed. The relationships for computing the radiation view factor of two equal size rectangles [15] were used for the current study since the base size of the heat sink tested was very close to the size of the hot surface. Also, the relationships for two parallel disks [19,20] could be used if the heat sink base size is different from the size of the

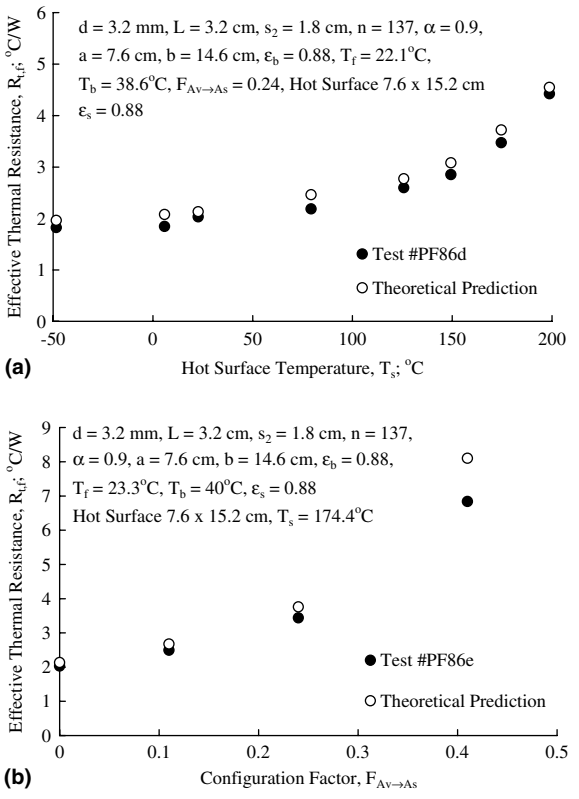

Fig. 5. Effects of radiation on thermal performance of heat sink fins operating in natural convection domain; (a) influence of a hot surface in the field of view of the heat sink, (b) influence of configuration factor.

hot surface. Since no relationship could be found for determining the radiation view factor for non-identical rectangles, an alternate method could be used to at least approximate it. This was done by finding an equivalent radius for each of the two parallel rectangles such that the area of the disk would equal the area of the rectangle.[6]

7.6. Experimental results

The influence of the hot surface temperature on the thermal performance of the fin array heat sink is shown in Fig. 5a with additional parameters in Table 1. As can be clearly seen from the graph of the experimental data, the thermal performance of the heat sink decreases considerably and non-linearly as the hot surface temperature increases above the ambient, but increases only slightly when the hot surface temperature is less than ambient. Therefore, the thermal radiation that is emitted from the hot surface and absorbed by the heat sink can cause a significant deterioration in the thermal performance.

Table 1
Experimental pin fin array thermal parameters for Fig. 5

Data set	T_b (°C)	T_f (°C)	ε
PF82a	37.6	22.4	0.1
PF82c	78.1	63.1	0.1
PF82d	37.5	23.1	0.88
PF82e	77.6	63.2	0.88

7.7. Predictive capability of the modified theoretical model

Also depicted in Fig. 5a is the theoretical prediction of the influence of thermal radiation on the thermal performance of the fin array heat sink using the theoretical model. The agreement appears to be quite good, especially knowing that there might be some errors in the estimation of some of the thermal radiation parameters such as the radiation view factor and emissivities.

7.8. Influence of radiation view factor on thermal performance of fin array heat sink

In order to investigate the influence of the radiation view factor on the thermal performance of the fin array heat sink, a test was run using the exact same apparatus shown in Fig. 2, and the fin array heat sink as described in the previous section. The hot surface was again heated with electrical patch heaters. The effective thermal resistance of the fin array heat sink for natural convection, $v_f = 0$ m/s, was measured as a function of the radiation view factor. The radiation view factor between the area of the heat sink in view of the hot surface, A_v, and the area of the hot surface, A_s, was varied by changing the distance between the hot surface and the tip of the fin array heat sink while holding the hot surface temperature constant. In these tests, the area of the heat sink array in view of the hot surface, A_v, was assumed to be the front face area of the fin array heat sink which was the same area as the heat sink base size as shown in Fig. 3. The radiation view factor was determined as explained earlier.

Fig. 5b depicts the influence of the radiation view factor on the thermal performance of the heat sink. It can be clearly seen that the thermal performance decreases considerably as the view factor increases. The reason for this is more of the thermal radiation leaving the hot surface strikes the heat sink as the view factor gets

[6] A comparison was made of the radiation view factors obtained using the equations for two equal size rectangles to those obtained for two parallel disks. It was found that they both gave similar values for the radiation view factor when the surface areas of the two rectangles and the two disks were the same.

larger, and the thermal radiation absorbed by the heat sink causes the deterioration in the thermal performance.

The theoretical prediction of the thermal performance, determined using the modified model, is also superimposed in Fig. 5b. The predictions are quite good when the view factor is relatively small. It is not as good when the view factor becomes larger. One of the reasons for this could be the error in the estimation of the radiation view factor. In the test, it was assumed that the area of the fin array heat sink in view of the hot surface, A_v, was the front face area of the heat sink which was the same area as the heat sink base size as shown in Fig. 3. In reality, however, as the view factor increases (that is, as the distance between the areas of the hot surface and the tip of the fin array heat sink gets shorter) the area of the heat sink in view of the hot surface, A_v, is actually slightly larger than the area of the front face of the heat sink since a part of the side face of the heat sink fins starts to become more important. The predictive capability of the modified theoretical model is seen to be quite good, again especially when consideration is given to the complexity of the various physical mechanisms involved, including combined mode convection and thermal radiation, as well as the difficulty in the determination of the parameters involved in the thermal radiation, such as the radiation view factors and the emissivities.

8. Design insight with respect to influence of thermal radiation

Using the modified theoretical model that has been developed, which includes the influence of thermal radiation, it is possible to extract some very useful design insights. Fig. 6a shows the predicted thermal performance in the form of the effective thermal resistance, $R_{t,s}$, of the fin array heat sink as a function of the velocity, v_f, for five different situations associated with the surfaces involved, with the radiation view factor between the area of fin array heat sink in view of the hot surface, A_v, and the hot surface, A_s, being $F_{A_v \to A_s} = 0.075$. The heat sink under consideration is the larger size heat sink that had a vertical base height, $a = 7.6$ cm, and a base width, $b = 14.6$ cm. The fin had a diameter, $d = 3.2$ mm, length, $L = 3.2$ cm, fin spacing, $s_2 = 1.8$ cm, and the number of fins, $n = 137$. The ambient air temperature, $T_f = 100$ °C. The emissivity of the polished aluminum surface and the dark surface were 0.1 and 0.88, respectively.

There are four different situations and one reference situation shown on the graphs. The reference situation is simply the best thermal performance situation where there is no hot surface in view of the heat sink, and thus no detrimental influence of the thermal radiation. Configuration A comprised of a dark fin array heat sink with

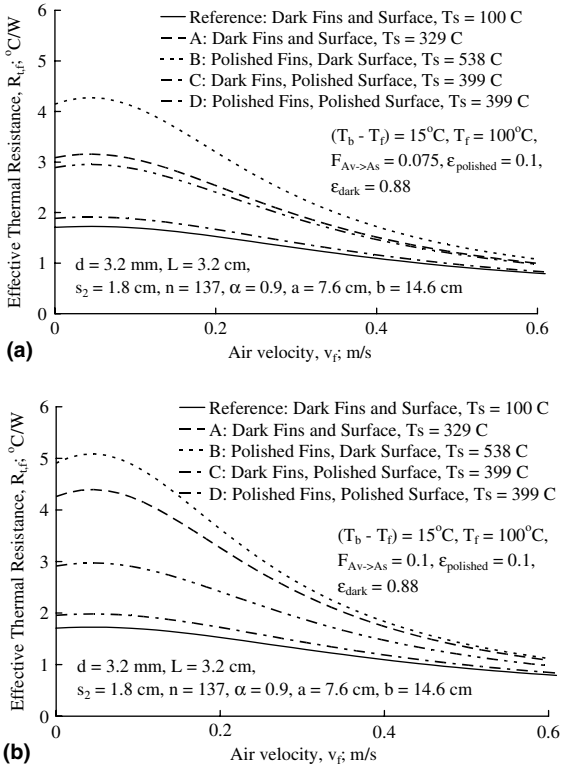

Fig. 6. Predicted thermal performance of heat sink fins; Comparison of the situations with various surfaces of heat sink Fins and hot surface and various hot surface temperature; (a) $F_{A_v \to A_s} = 0.075$, (b) $F_{A_v \to A_s} = 0.1$.

a dark hot surface at a temperature, $T_s = 329.4$ °C. Configuration B involved a polished aluminum fin array heat sink with a dark hot surface at a temperature, $T_s = 537.8$ °C. Configuration C included a dark fin array heat sink with a polished aluminum hot surface at a temperature, $T_s = 398.9$ °C. Configuration D included a polished aluminum finned heat sink with a hot surface polished aluminum and at a temperature, $T_s = 398.9$ °C. Figs. 6b and 7 are identical to Fig. 6a except that the radiation view factor, $F_{A_v \to A_s}$, is increased to 0.1 and 0.15, respectively. Notable between these figures is the dramatic detrimental increase in thermal resistance as $F_{A_v \to A_s}$ increases.

As can be seen in Figs. 6 and 7, the influence of the different radiation configurations is considerable in the natural convection domain. Also, when a hot surface is in view of the heat sink, the fin array heat sink performs the best when the fins are black and the hot surface is polished aluminum. This would correspond to the situation where the hot surface in view of the heat sink was a polished heat shield in front of an even hotter surface. The reason the dark fin array heat sink performs better than the polished aluminum is because the thermal radiation leaving the dark fin array heat sink to

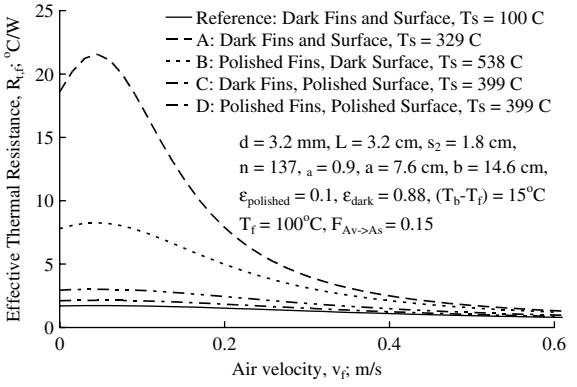

Fig. 7. Predicted thermal performance of heat sink fins; comparison of the situations with various surfaces of heat sink fins and hot surface and various hot surface temperature; $F_{A_v \to A_s} = 0.15$.

the environment is much greater than the thermal radiation leaving the polished aluminum finned heat sink to the environment. Moreover, since the radiation view factor between the heat sink fins and the hot surface is small, the thermal radiation leaving the hot surface to the fin array heat sink is less than the radiation leaving the fins to the rest of the environment. If the radiation view factor between the fin array heat sink and the hot surface gets high enough, ($F_{A_v \to A_s} \geqslant 0.35$), then for the particular conditions represented in any of these three figures, the polished aluminum fin array heat sink would perform equal to or better than the dark heat sink fins.

9. Summary and conclusions

A theoretical and experimental study of the influence of thermal radiation has been carried out on the thermal performance of a fin array heat sink. The focus of the study has resulted in the successful development of a theoretical thermal radiation model that has the capability for predicting the magnitude of the influence of thermal radiation on the effective thermal resistance of a fin array heat sink. The thermal radiation model is formulated in such a way that it complements the theoretical model developed earlier for natural and combined forced and natural convection [10]. This was done by developing an effective radiation heat transfer coefficient that can simply be added to the convective heat transfer coefficient. The value of the theoretical model, which now includes the influence of thermal radiation on the thermal performance, is that it can be used as a significant design tool to determine the influence of various design parameters on the effective thermal resistance of the heat sink, such as fin diameter, length, spacing, and emissivity, base size, orientation, and temperature, air flow velocity and temperature, hot surface temperature and emissivity, and radiation view factor between the heat sink fins and the hot surface. Experimental validation of the theoretical model for the parameters involved in thermal radiation has been carried out for pure natural convection, and for combined natural and forced convection. The range of parameters for the theoretical model is the same as described in the previous section.

The results of a parametric study utilizing the modified theoretical model lead to the conclusion that fin array heat sinks perform the best when they are flat black, and the hot surface is polished aluminum, assuming that the view factor between the two surfaces is small. This would correspond to the situation where the hot surface in view of the heat sink would be a polished heat shield in front of an even hotter surface. If there is no hot surface in view of the heat sink, flat black fins still provide the best thermal performance.

Acknowledgements

The authors would like to acknowledge M.C. Cwiek and R. Saxena, of core electronics, LCP Engineering, for their technical support and encouragement. Acknowledgment is also given to Stu Dorsey and Frank Cox of the Oakland University Instrument Shop for their expertise in constructing the many different heat sink configurations used in the experimental phase of the research. This research was sponsored, in part, by Chrysler Corporation.

References

[1] G. Ledezma, A.M. Morega, A. Bejan, Optimal spacing between pin fins with impinging flow, ASME J. Heat Transfer 118 (1996) 570–577.
[2] E.M. Sparrow, E.D. Larson, Heat transfer from pin-fins situated in an oncoming longitudinal flow which turns to crossflow, Int. J. Heat Mass Transfer 25 (5) (1982) 603–614.
[3] K. Minakami, K. Hisano, H. Iwasaki, S. Mochizuki, Application of the pin-fin heat sink to electronic equipment (Study on design method for flow-guide vanes), CAFJ-CAD Application to Electronic Packaging ASME, EEP-18, 1996, pp. 117–122.
[4] E.W. Constans, A.D. Belegundu, A.K. Kulkarni, Optimization of a pin-fin sink: A design tool, CAFJCAD Application to Electronic Packaging ASME, EEP-9, 1994, pp. 25–32.
[5] H.I. You, C.H. Chang, Numerical prediction of heat transfer coefficient for a pin-fin channel flow, ASME J. Heat Transfer 119 (1997) 840–843.
[6] C.L. Chapman, S. Lee, B.L. Schmidt, Thermal performance of an elliptical pin fin heat sink, in: Tenth Annual IEEE Semiconductor Thermal Measurement and Management Symposium, 1994, pp. 24–31.

[7] K. Minakarni, M. Ishizuka, S. Mochizuki, Performance evaluation of pin-fin heat sinks utilizing a local heating method, J. Enhanc. Heat Transfer 2 (1–2) (1995) 17–22.
[8] Y. Kondo, H. Matsushima, Prediction algorithm of thermal resistance in the case of pin-fin heat sinks for LSI packages using impingement cooling, Nihon Kikai Gakkai Ronbunshu (B-hen) 62 (595) (1996) 332–339.
[9] W.W. Lin, D.J. Lee, Second-law analysis on a pin-fin array under crossflow, Int. J. Heat Mass Transfer 40 (8) (1997) 1937–1945.
[10] C.J. Kobus, T. Oshio, Development of a theoretical model for predicting the thermal performance characteristics of a vertical pin-fin array heat sink under combined forced and natural convection with impinging flow, Int. J. Heat Mass Transfer 48 (6) (2005) 1053–1063.
[11] V.R. Rao, S.P. Venkateshan, Experimental study of free convection and radiation in horizontal fin arrays, Int. J. Heat Mass Transfer 39 (4) (1996) 779–789.
[12] E.M. Sparrow, S.B. Vemuri, Natural convection–radiation heat transfer from highly populated pin-fin arrays, ASME J. Heat Transfer 107 (1985) 190–197.
[13] E.M. Sparrow, S.B. Vemuri, Orientation effects on natural convection/radiation pin-fin arrays, Int. J. Heat Mass Transfer 29 (1986) 359–368.
[14] T. Aihara, S. Maruyama, S. Kobayakawa, Free convective/radiative heat transfer from pin-fin arrays with a vertical base plate (general representation of heat transfer performance), Int. J. Heat Mass Transfer 33 (6) (1990) 1223–1232.
[15] E. Yu, Y. Joshi, Heat transfer enhancement from enclosed discrete components using pin-fin heat sinks, Int. J. Heat Mass Transfer 45 (25) (2002) 4957–4966.
[16] E. Yu, Y. Joshi, Heat transfer in discretely heated side-vented compact enclosures by combined conduction, convection, and radiation, ASME J. Heat Transfer 121 (1999) 1002–1010.
[17] M. Sasikumar, C. Balaji, A holistic optimization of convecting–radiating Fin systems, ASME J. Heat Transfer 124 (6) (2002) 1110–1116.
[18] D.S. Gerencser, A. Razani, Optimization of radiative-convective arrays of pin fins including mutual irradiation between Fins, Int. J. Heat Mass Transfer 38 (5) (1995) 899–907.
[19] R. Siegel, J.R. Howell, Thermal Radiation Heat Transfer, second ed., McGraw-Hill, New York, 1981, p. 824.
[20] R. Siegel, J.R. Howell, Thermal Radiation Heat Transfer, second ed., McGraw-Hill, New York, 1981, p. 826.